Heat Mass Transfer (2008) 44:1005–1013
DOI 10.1007/s00231-007-0340-x

ORIGINAL

Buoyant MHD flows in a vertical channel: the levitation regime

A. Barletta · M. Celli · E. Magyari · E. Zanchini

Received: 21 May 2007 / Accepted: 28 August 2007 / Published online: 14 September 2007

Abstract Buoyant magnetohydrodynamic (MHD) flows with Joulean and viscous heating effects are considered in a vertical parallel plate channel. The applied magnetic field is uniform and perpendicular to the plates which are subject to *adiabatic* and *isothermal* boundary conditions, respectively. The main issue of the paper is the *levitation regime*, i.e., the fully developed flow regime for large values of the Hartmann number M, when the hydrodynamic pressure gradient evaluated at the temperature of the adiabatic wall is vanishing. The problem is solved analytically by Taylor series method and the solution is validated numerically. It is found that the fluid velocity points everywhere and for all values of M downward. For small M's, the velocity field extends nearly symmetrically (with respect to the mid-plane) over the whole section of the channel between the adiabatic and the isothermal walls. For large values of M, by contrast, the fluid levitates over a broad transversal range of the channel, while the motion becomes concentrated in a narrow boundary layer in the neighborhood of the isothermal wall. Accordingly, the fluid temperature is nearly uniform in the levitation range and decreases rapidly within the boundary layer in front of the isothermal wall. It also turns out that not only the volumetric heat generation by the Joule effect, but also that by viscous friction increases rapidly with increasing values of M, the latter effect being even larger than the former one for all M.

A. Barletta · M. Celli · E. Magyari · E. Zanchini
Dipartimento di Ingegneria Energetica,
Nucleare e del Controllo Ambientale (DIENCA),
Università di Bologna, Via dei Colli 16,
40136 Bologna, Italy

E. Magyari (✉)
Institute of Building Technology,
ETH-Zurich, Switzerland
e-mail: magyari@hbt.arch.ethz.ch

List of symbols

A	series coefficients, (28)
$\mathbf{B}$	applied magnetic field
$\mathbf{f}$	magnetohydrodynamic force, (2)
g	acceleration of gravity
$\mathbf{J}$	electric current density, (1)
k	fluid thermal conductivity
L	channel width
M	Hartmann number, (21)
p	pressure
P	hydrodynamic pressure
q	dimensionless heat flux
$\bar{q}$	dimensional heat flux
$\dot{Q}$	rate of volumetric heat generation
T	temperature
u	dimensionless velocity, (21)
u_m	dimensionless average velocity
U	velocity
U_0	velocity scale, (20)
X	vertical coordinate
Y	transversal coordinate
y	dimensionless transversal, (20)

Greek symbols

α	slope parameter, (31)
β	thermal coefficient of volumetric expansion of the fluid
μ	dynamic viscosity
υ	kinematic viscosity ($\upsilon = \mu/\rho$)
ρ	mass density of the fluid
σ	electrical conductivity

θ dimensionless temperature, (21)
ΔT temperature scale, (20)

Subscripts, superscripts

m average value
n, j running indices
primes differentiation with respect to the argument

1 Introduction

The broad research interest in magnetohydrodynamic (MHD) flows of electrically conducting fluids in ducts and enclosures is motivated by their important industrial applications in metallurgy and in growing of pure crystals, as well as in energy engineering. In an earlier work of Potts [1] the fully developed flow in a vertical channel with isothermal walls and an applied transversal magnetic field was investigated in some detail. Later on, Setayesh and Sahai [2] consider the effect of the temperature dependent transport properties on the MHD channel flow. The simultaneous effect of the Joulean and viscous heating on the channel flow under isothermal boundary conditions has been examined analytically and numerically by Umavathi [3] and Umavathi and Malashetty [4] by applying perturbation methods. The flow in strong magnetic field in rectangular ducts has been investigated by Bühler [5] and results on the Rayleigh–Benard convection in a vertical magnetic field were reported by Burr and Müller [6]. The oscillatory instability of MHD flows in rectangular cavities has been analyzed by Gelfgat and Bar-Yoseph [7]. In a more recent paper by Sposito and Ciofalo [8] the fully developed mixed convection flow in vertical rectangular duct has been examined under various boundary conditions of practical interest.

The aim of the present paper is to investigate the *levitation regime* of the MHD flow in a vertical channel whose walls are subject to adiabatic and isothermal boundary conditions, respectively. The levitation regime is reached for large values of the Hartmann number M, when the hydrodynamic pressure gradient of the fully developed flow, evaluated at the temperature of the adiabatic wall, becomes zero. To our knowledge, this regime of the MHD channel flow was not investigated until now. The mechanical and thermal characteristics of the flow in the levitation regime are examined in the paper analytically and numerically in detail.

2 Governing equations

2.1 Problem formulation

We consider the steady laminar flow of an electrically conducting fluid of electric conductivity σ in a vertical parallel plane channel of width L. The X-axis of the coordinate system is opposite to the acceleration due to the gravity $\mathbf{g}$ and the Y-axis is perpendicular to the channel walls which are assumed to be impermeable (see Fig. 1). The left wall (at $Y = 0$) is insulated (adiabatic wall) and the right one (at $Y = L$) is kept at the constant temperature T_w (isothermal wall). A uniform external magnetic field $\mathbf{B}$ is applied perpendicularly to the channel walls. No external electric field acts and it is assumed that, comparing to the external magnetic field, the magnetic field induced by the moving fluid is negligibly weak. Under these conditions, the Lorentz force $e(\mathbf{v}\times\mathbf{B})$ acting on a fluid element of electric charge e and velocity $\mathbf{v}$, will be experienced by the fluid element in its own reference frame as the effect of an electric field $\mathbf{E} = \mathbf{v}\times\mathbf{B}$. This latter field gives rise to an electric current of density $\mathbf{J}$ which, according to Ohm's law, is obtained as

$$\mathbf{J} = \sigma\mathbf{E} = \sigma(\mathbf{v}\times\mathbf{B}) \tag{1}$$

The interaction of $\mathbf{J}$ with the applied magnetic field $\mathbf{B}$ causes in turn a magnetohydrodynamic force of volume density $\mathbf{f} = \mathbf{J}\times\mathbf{B} = \sigma(\mathbf{v}\times\mathbf{B})\times\mathbf{B}$, which can be transcribed in the form

$$\mathbf{f} = \sigma\left[(\mathbf{v}\cdot\mathbf{B})\mathbf{B} - B^2\mathbf{v}\right] \tag{2}$$

The rate of the volumetric heat generation by the Joule effect, $\dot{Q}_{\text{Joule}} = \mathbf{J}\cdot\mathbf{E}$, is given according to (1) by

$$\dot{Q}_{\text{Joule}} = \sigma|\mathbf{v}\times\mathbf{B}|^2 \tag{3}$$

Furthermore, we assume that the flow is fully developed and parallel, the only non-vanishing component of the velocity field being its X-component U, i.e., $\mathbf{v} = U\mathbf{e}_\mathbf{x}$, where

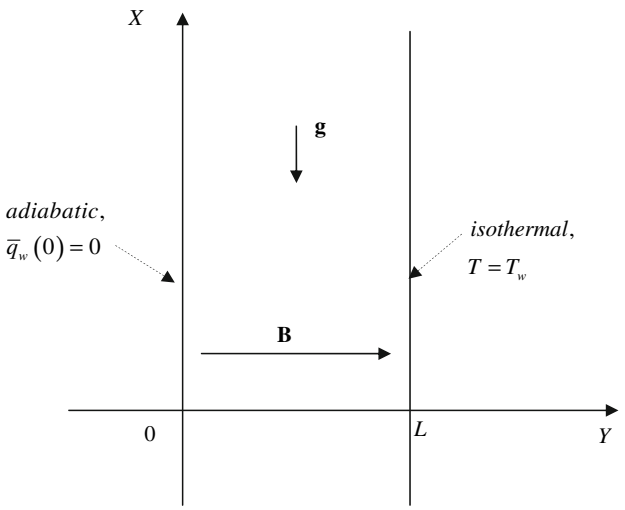

Fig. 1 Coordinate system, applied magnetic filed **B**, and adiabatic and isothermal boundary conditions at $Y = 0$ and $Y = L$, respectively

$\mathbf{e_x}$ denotes the unit vector of the positive X-axis. This flow regime is established in long channels far downstream from the inlet section. As a consequence, (2) and (3) reduce to

$$\mathbf{f} = -\sigma B^2 U \mathbf{e_x}, \quad \dot{Q}_{\text{Joule}} = \sigma B^2 U^2 \tag{4}$$

We assume that the Boussinesq approximation holds and that, in addition to the Joulean heating, the volumetric heat generation by viscous friction is also significant. Under all these assumptions, both the velocity U and the temperature T of the fluid depend only on the transversal coordinate Y, the continuity equation is satisfied identically, the transversal component of the hydrodynamic pressure gradient $\partial P/\partial Y$ is vanishing, the planar one, $\partial P/\partial X$ is (a given) constant, the velocity and temperature gradients along the x-axis are identically vanishing, and the momentum and energy equations become

$$-\frac{dP}{dX} + \mu\frac{d^2U}{dY^2} - \sigma B^2 U + \rho g\beta[T - T(0)] = 0 \tag{5}$$

$$k\frac{d^2T}{dY^2} + \sigma B^2 U^2 + \mu\left(\frac{dU}{dY}\right)^2 = 0 \tag{6}$$

The no slip conditions and the prescribed thermal boundary conditions read

$$U(0) = U(L) = 0 \tag{7}$$

$$-k\left.\frac{dT}{dY}\right|_{Y=0} = \bar{q}(0) = 0, \quad T(L) = T_w \tag{8}$$

In the above equations, $P = p + \rho g X$ denotes the hydrodynamic pressure. The magnitude B of the applied magnetic field is given and the values of ρ, μ, β, k and σ are taken at the reference temperature of the Boussinesq approximation T_{ref} which, following Morton [11], has been chosen equal to the temperature $T(0)$ of the insulated wall, $T_{\text{ref}} = T(0)$. We are interested in the *levitation regime* of the flow which is reached in strong magnetic field, when the hydrodynamic pressure gradient evaluated at the temperature of the adiabatic wall is vanishing,

$$\frac{dP}{dX} = 0 \tag{9}$$

In this physical situation the difference between the pressure p and the hydrostatic pressure $\rho\, g\, X$ with $\rho = \rho|_{T=T_{\text{ref}}}$ is the same constant quantity at all stations X of the fully developed flow.

2.2 Solution procedure

The basic idea of the solution procedure is to first determine the velocity field $U = U(Y)$ and to express then all the quantities of physical and engineering interest in terms of U. Thus the, temperature $T(Y)$ as expressed in terms of U from (5) is

$$T(Y) = T(0) + \frac{\mu}{\rho g\beta}\left(\frac{\sigma B^2}{\mu}U - \frac{d^2U}{dY^2}\right) \tag{10}$$

Accordingly, the flux field $\bar{q}(Y) = -k dT/dY$ is obtained as

$$\bar{q}(Y) = \frac{k\mu}{\rho g\beta}\left(\frac{d^3U}{dY^3} - \frac{\sigma B^2}{\mu}\frac{dU}{dY}\right) \tag{11}$$

Substituting (10) in (6) we obtain for the velocity U the explicit non linear ordinary differential equation of the fourth order,

$$\frac{d^4U}{dY^4} = \frac{\sigma B^2}{\mu}\left(\frac{d^2U}{dY^2} + \frac{\rho g\beta}{k}U^2\right) + \frac{\rho g\beta}{k}\left(\frac{dU}{dY}\right)^2 \tag{12}$$

Having in mind (10) and (11), the boundary conditions (7) and (8) yield the following two differential conditions for the velocity U

$$\left.\frac{d^2U}{dY^2}\right|_{Y=0} = 0 \tag{13}$$

$$\left.\frac{d^3U}{dY^3}\right|_{Y=0} - \left.\frac{\sigma B^2}{\mu}\frac{dU}{dY}\right|_{Y=0} = 0 \tag{14}$$

Thus, the fourth order differential equation (12) along with the four conditions (8), (13) and (14) specify a closed two point boundary value problem for the velocity field. The solution of this problem is the main objective of Sect. 3. Therefore, anticipating that (for specified B) the solution $U = U(Y)$ is known, (10) and the second boundary condition (8) give for the temperature $T(0)$ of the adiabatic wall the expression

$$T(0) = T_w + \left.\frac{\mu}{\rho g\beta}\frac{d^2U}{dY^2}\right|_{Y=L} \tag{15}$$

Furthermore, (16) and (15) yield the temperature field

$$T(Y) = T_w + \frac{\mu}{\rho g\beta}\left(\frac{\sigma B^2}{\mu}U + \left.\frac{d^2U}{dY^2}\right|_{Y=L} - \frac{d^2U}{dY^2}\right) \tag{16}$$

in terms of known quantities. The outgoing heat flux $\bar{q}(L)$ through the isothermal wall is obtained immediately by substituting $Y = L$ in (11),

$$\bar{q}(L) = \frac{k\mu}{\rho g\beta}\left(\left.\frac{d^3U}{dY^3}\right|_{Y=L} - \left.\frac{\sigma B^2}{\mu}\frac{dU}{dY}\right|_{Y=L}\right) \tag{17}$$

In addition to the above equations, a further relationship of physical interest is the integral balance equation of the heat fluxes

$$\bar{q}(L) = \bar{q}_{\text{Joule}} + \bar{q}_{\text{Viscous}} \tag{18}$$

where

$$\bar{q}_{\text{Joule}} = \sigma B^2 \int_0^L U^2 dY \text{ and } \bar{q}_{\text{viscous}} = \mu \int_0^L \left(\frac{dU}{dY}\right)^2 dY \tag{19}$$

are the heat fluxes due to the volumetric heat generation by Joulean and viscous heating effects, respectively. Equation (18), which has been obtained by integration of the energy equation (6), shows that the outgoing heat flux through the isothermal wall equals, as expected, the sum of the heat fluxes $\bar{q}_{\text{Joule}}$ and $\bar{q}_{\text{Viscous}}$ due to the two simultaneous volumetric heat generation effects. The latter two quantities can be calculated from (19), once the velocity field is known. In this way the problem has basically been solved.

2.3 Nondimensionalization

For our present purpose it is convenient to choose the velocity and temperature scales

$$U_0 = \frac{k}{\rho g \beta L^2}, \quad \Delta T = \frac{\mu U_0^2}{k} \tag{20}$$

In terms of the dimensionless quantities

$$y = M\frac{Y}{L}, \quad u(y) = \frac{1}{M^2}\frac{U(Y)}{U_0}, \quad \theta(y) = \frac{T(Y) - T_w}{\Delta T},$$
$$q(y) = \frac{L}{k\Delta T}\bar{q}(Y), \quad M = \sqrt{\frac{\sigma}{\mu}}BL \tag{21}$$

where M stands for the Hartmann number, (12) and the associated boundary conditions (7), (13) and (14) become

$$u'''' = u'' + u'^2 + u^2, \tag{22}$$

$$u(0) = 0, \quad u(M) = 0, \quad u''(0) = 0, \quad u'''(0) = u'(0) \tag{23}$$

Here the primes denote differentiations with respect to y.

The solution of the two point boundary value problem (22), (23) yields the dimensionless velocity field $u = u(y)$ for a specified value of M. Then, in terms of this solution $u = u(y)$,

we obtain from (16) and (21) the dimensionless temperature field

$$\theta(y) = M^4[u(y) - u''(y) + u''(M)] \tag{24}$$

and from (17) the dimensionless flux field

$$q(y) = M^5[u'''(y) - u'(y)] = -M\theta'(y) \tag{25}$$

Similarly, (18) and (19) go over into the dimensionless forms

$$q(1) = q_{\text{Joule}} + q_{\text{Viscous}} \tag{26}$$

$$q_{\text{Joule}} = M^5 \int_0^M u^2 dy, \quad q_{\text{viscous}} = M^5 \int_0^M u'^2 dy \tag{27}$$

Equations (22) and (23) reveal a remarkable feature of the levitating flows. Namely, the flows corresponding to different values of the Hartmann number M, possess the same *universal velocity profile* u = $u(y)$, when are observed in channels of the respective dimensionless widths M. It is also worth mentioning here that, this property holds not only on the special velocity and temperature scales (20), but on all scales. The choice (20) has been privileged since it implies for the ratio of the Grashof and Reynolds numbers $Gr = g\beta L^3 \Delta T/\upsilon^2$ and $\text{Re} = U_0 L/\upsilon$, as well as for the Brinkman number $Br = \mu U_0^2/(k\Delta T)$, the value unity, $Gr/Re = Br = 1$.

3 Power series solution

The aim of this section is to give an analytical power series solution of the boundary value problem (22), (23). To this end, we first formally expand the function $u(y)$ in a Taylor series to powers of y,

$$u(y) = \sum_{n=0}^{\infty} A_n y^n \tag{28}$$

Substituting (28) in (22) and identifying the coefficients of the same powers of y, we obtain the recurrence equations

$$A_{n+4} = \frac{A_{n+2}}{(n+3)(n+4)} + \frac{\sum_{j=0}^{n}\left[A_j A_{n-j} + (j+1)(n-j+1)A_{j+1}A_{n-j+1}\right]}{(n+1)(n+2)(n+3)(n+4)}, \quad n = 0, 1, 2, \ldots \tag{29}$$

which allows us to determine all the coefficients A_4, A_5, A_6, ... in terms of the first four ones, A_0, A_1, A_2 and A_3. Having in mind that the coefficients A_n are related to the derivatives of $u(y)$ at $y = 0$ by the relationship

$$A_n = \frac{u^{(n)}(0)}{n!}, \tag{30}$$

and introducing the notation

$$u'(0) = \alpha \tag{31}$$

we obtain from (23) the following expressions for the first four coefficients of series (28),

$$A_0 = 0, \quad A_1 = \frac{\alpha}{1!}, \quad A_2 = 0, \quad A_3 = \frac{\alpha}{3!} \tag{32}$$

Therefore, the coefficients of the series (28) depend only on the unknown parameter α, $A_n = A_n(\alpha)$. The next coefficients obtained from (29) and (32) are

$$A_4 = \frac{\alpha^2}{4!}, \; A_5 = \frac{\alpha}{5!}, \; A_6 = \frac{5\alpha^2}{6!}, \; A_7 = \frac{2\alpha^3 + \alpha}{7!},$$
$$A_8 = \frac{21\alpha^2}{8!}, \; A_9 = \frac{42\alpha^3 + \alpha}{9!}, \; A_{10} = \frac{24\alpha^4 + 85\alpha^2}{10!},$$
$$A_{11} = \frac{504\alpha^3 + \alpha}{11!}, \; A_{12} = \frac{882\alpha^4 + 341\alpha^2}{12!}, \ldots \tag{33}$$

The parameter α represents according to (31) the slope $u'(0)$ of the dimensionless velocity profile $u(y)$ at the insulated wall $y = 0$. The value of α has to be determined from the second boundary condition (23) which transcribes to

$$u(M) \equiv u(M;\alpha) = \sum_{n=0}^{\infty} A_n(\alpha) M^n = 0 \tag{34}$$

In this way the two point boundary value problem (22), (23) can also be viewed as an initial value problem for (22), with the initial conditions

$$u(0) = 0, \quad u'(0) = \alpha, \quad u''(0) = 0, \quad u'''(0) = \alpha, \tag{35}$$

whose solution is subject to the additional condition (34).

The advantage of this reformulation of the original problem (22), (23) resides in two important features, namely, (1) the solution of the initial value problem (22), (35) does exist for any specified value of the parameter α, and (2) the solution is unique. In this way, the existence and uniqueness of the solutions of the original two-point boundary value problem (22), (23) can be decided (for any finite value of M) with the aid of the additional condition (34). Once the value of α is determined, the solution of our velocity boundary value problem can be obtained from the series solution (28) as follows

$$\frac{U(Y)}{U_0} = M^2 u(y) = M^2 \sum_{n=0}^{\infty} A_n(\alpha) \left(M \frac{Y}{L} \right)^n \tag{36}$$

Then, $\theta(y)$, $q(y)$, q_{Joule} and q_{viscous} can be calculated by substituting the series (28) into (24)–(27). In addition, the average velocity U_m through a transversal section of the channel is obtained as

$$\frac{U_m}{U_0} = \frac{1}{L} \int_0^L \frac{U(y)}{U_0} dY = M^2 \sum_{n=0}^{\infty} \frac{A_n M^n}{n+1} \tag{37}$$

In this way the problem has been solved explicitly.

4 Discussion

4.1 Mechanical characteristics

The explicit expression (36) of the velocity field includes via A_n the parameter α which represents (from geometrical point of view) the slope $u'(0)$ of the scaled velocity profile $u(y)$ at the insulated wall $y = 0$. From mechanical point of view, the value of α specifies the (scaled) skin friction of the flow at the adiabatic channel wall. The remaining problem is to determine the value of α which, for a specified M, is obtained as root of (34). The main features of the roots of (34) become manifest by a simple inspection of Fig. 2a which shows the following.

- $\alpha = 0$ is a root of (34) for any value of the Hartmann number M. This trivial solution corresponds to the static equilibrium state of the system.
- There exists a unique non trivial root $\alpha_0 = \alpha_0(M) < 0$ of (34) for any given $M > 0$. Accordingly, the velocity solution (36) corresponding to the levitating flow is unique for any given $M > 0$.
- The root $\alpha_0(M)$ moves toward $-\infty$ as $M \to 0$, and approaches zero as $M \to \infty$ (see Fig. 2b). For instance, $\alpha_0(0.1) = -28888$ and $\alpha_0(10) = -0.001139$ (these cases are not included in Fig. 2a, b).

The dimensionless velocity profiles $U(Y)/U_0 = M^2 u(y)$ corresponding to the "small" values $M = 0.9, 1.0, 1.2$ and 1.5 of the Hartmann number (already selected for Fig. 2a), are plotted as functions of Y/L in Fig. 3a. In addition, in Fig. 3a also the solution corresponding to the case $M = 0$ has been included, which, on the scale $\tilde{y} = Y/L$ of the function $U(Y)/U_0 = \tilde{u}(\tilde{y})$, corresponds to the value $\tilde{\alpha} = -28.8781$ of the slope parameter $\tilde{\alpha}$ (for details see Appendix A). Furthermore, Fig. 3b shows the profiles $U(Y)/U_0 = M^2 u(y)$ for the "large" values $M = 3, 5, 8$ and 10 of the Hartmann number. One sees that the fluid velocity points everywhere and for all values of M in the downward direction. With respect to the mid-plane of the channel, the velocity field extends nearly symmetrically over the whole section of the channel between the adiabatic and the isothermal wall, as long as the Hartmann number is small (Fig. 3a). The minima of these small-M profiles are shifted only slightly toward the isothermal wall. For instance, $(Y_{\min}/L = 0.612154, U_{\min}/U_0 = -13.0742)$ for $M = 0$, and

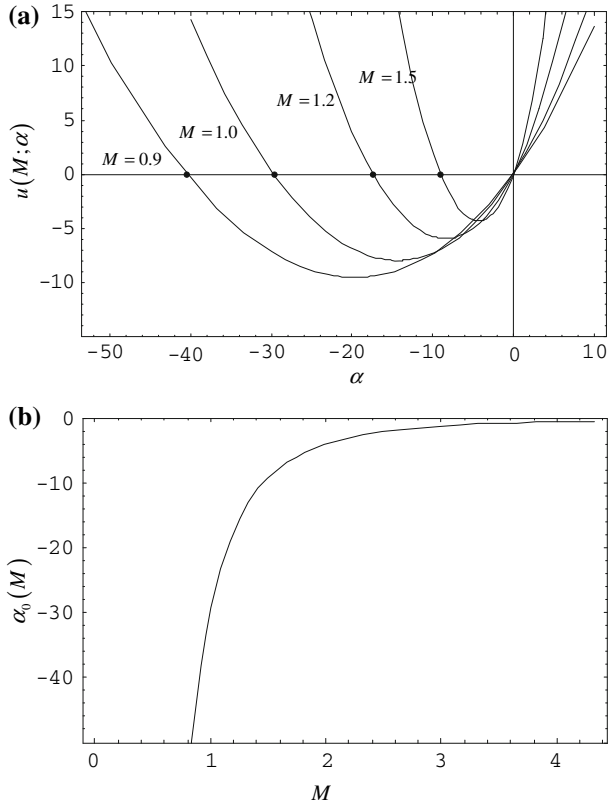

Fig. 2 **a** Plot of $u(M;\alpha)$ as a function of the parameter α according to (34) for four different values of the Hartmann number M. The dots on the α-axis mark the corresponding roots $\alpha_0 = \alpha_0(M)$ of equation $u(M;\alpha) = 0$; $\alpha_0(0.9) = -40.58$; $\alpha_0(1.0) = -29.72$; $\alpha_0(1.2) = -17.38$; $\alpha_0(1.5) = -9.04$. **b** Plot of the root $\alpha_0 = \alpha_0(M) < 0$ of (34) as a function of the Hartmann number

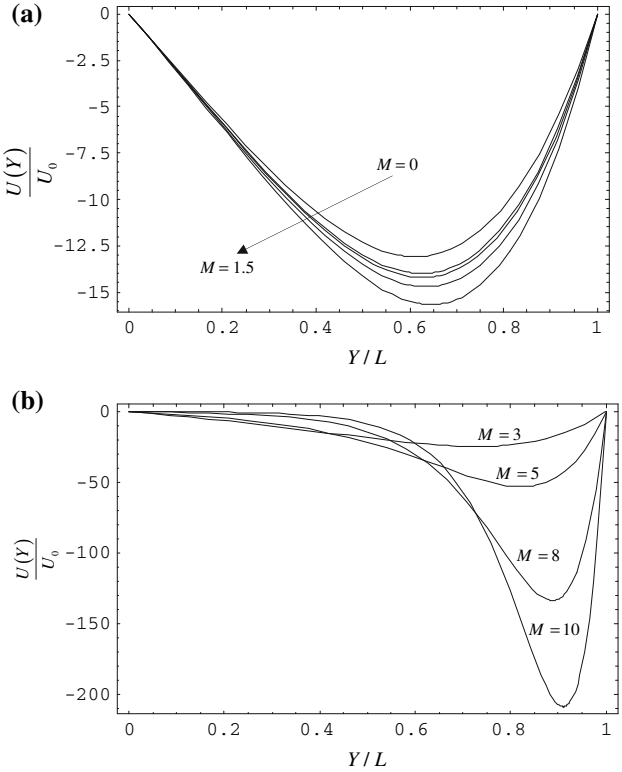

Fig. 3 **a** Plots of the dimensionless velocity profiles $U(Y)/U_0 = M^2u(y)$ as functions of Y/L for $M = 0.9$, 1.0, 1.2 and 1.5, and of $U(Y)/U_0 = \tilde{u}(\tilde{y})$ as a function of $\tilde{y} = Y/L$ for $M = 0$ (see Appendix A). **b**: Plots of the dimensionless velocity profiles $U(Y)/U_0 = M^2u(y)$ as functions of Y/L for $M = 3$, 5, 8 and 10

($Y_{min}/L = 0.646112, U_{min}/U_0 = -15.6549$) for $M = 1.5$. However, with increasing values of M, the velocity field undergoes a dramatic change, namely the fluid levitates over a large transversal range of the channel, while the motion becomes concentrated in a narrow boundary layer in the neighborhood of the isothermal wall (Fig. 3b). The larger M, the thinner the velocity boundary layer, and the larger the levitation range. The average velocity (volumetric flow rate) given by (37) also decreases with increasing values of M rapidly. For instance, $U_m/U_0 = -8.87$ for $M = 0.9$, and $U_m/U_0 = -47.47$ for $M = 10$.

4.2 Thermal characteristics

The main thermal characteristics of the levitating flows are illustrated for "small" and "large" values of the Hartmann number in Figs. 4, 5 and 6. Figure 4a and b show the dimensionless temperature profiles $\theta = \theta(y)$ and Fig. 5a and b the corresponding heat fluxes within the flow, respectively. The physical correlation between these figures on the one hand, and the velocity profiles shown in Fig. 3a and b on the other hand, becomes immediately evident. Indeed, for small values of M, where the velocity field extends nearly symmetrically over the whole section of the channel (Fig. 3a), the temperature decreases gradually from the maximum value $\theta(0)$ reached at the adiabatic wall, to the value zero at the isothermal wall (Fig. 4a). At the same time the total heat flux generated by Joulean and viscous heating increases continuously from zero at the adiabatic wall, to the maximum value reached at the isothermal wall (Fig. 5a). For large values of M, by contrast, in the transversal range of the channel where the fluid levitates (Fig. 3b), the temperature is almost uniform (Fig. 4b) and the transversal heat flux is (nearly) vanishing (Fig. 5b). However, across the boundary layer next to the isothermal boundary, both the fluid temperature and the heat flux experience a steep change with increasing M. The rapid increase of the heat flux near to the isothermal wall (Fig. 5b) is due to the intense heat generation by Joulean and viscous heating within the boundary layer (Fig. 6b). It is worth emphasizing here again that with increasing value of the Hartmann number, not only the volumetric heat generation by the Joule effect, but also that by viscous friction increases rapidly. The latter effect is even stronger than the former one (see Fig. 6a, b).

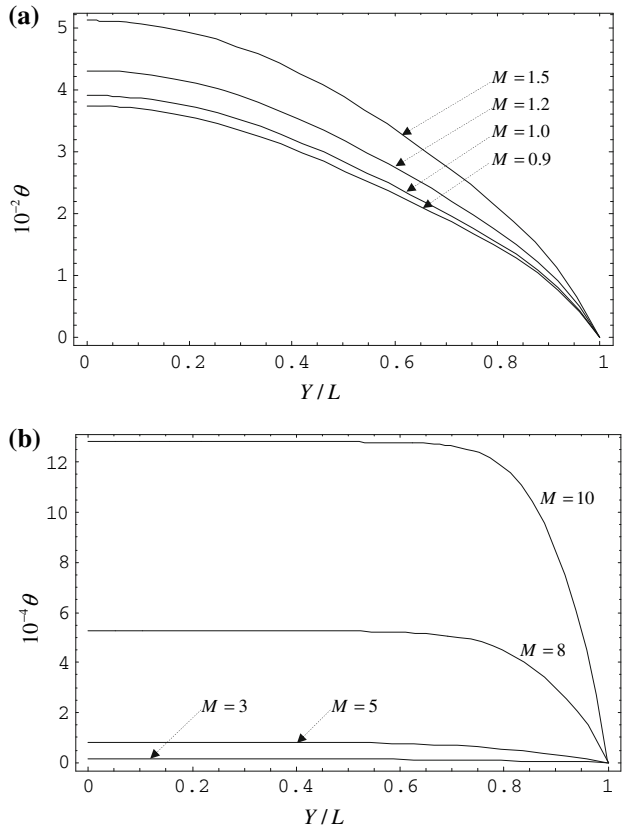

Fig. 4 **a** Plots of the dimensionless temperature profiles θ (y) according to (24) (multiplied 10^{-2}) for M = 0.9, 1.0, 1.2 and 1.5. **b** Plots of the dimensionless temperature profiles θ (y) according to (24) (multiplied by 10^{-4}) for M = 3, 5, 8 and 10

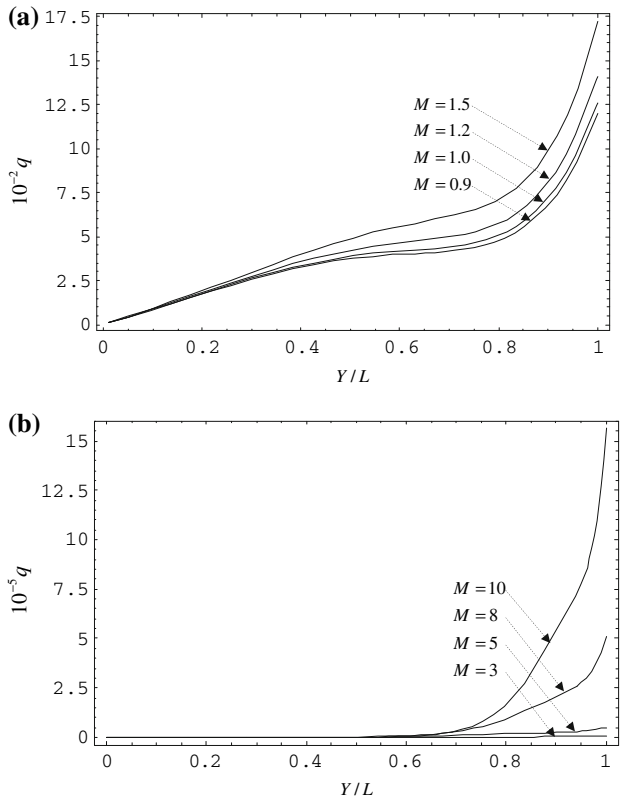

Fig. 5 **a** Plots of the dimensionless heat fluxes $q(y)$ according to (25) (multiplied by 10^{-2}) for M = 0.9, 1.0, 1.2 and 1.5. **b** Plots of the dimensionless heat fluxes $q(y)$ according to (25) (multiplied by 10^{-5}) for M = 3, 5, 8 and 10

4.3 Convergence acceleration and validation of results

A shortcoming of power series solutions of differential equations consists often in their slow convergence, which requires that in their practical use a large number of terms must be considered. This may cause in turn steeply increasing computational times. In the case of Taylor series solution reported in Sect. 3, this problem may also arise for large values of the slope parameter α (see e.g., Eqs. (33)). The convergence can sometimes be accelerated with the aid of the classical Euler–Knopp type series transformation [9]. In the present calculations, following the work of Gabutti and Lyness [10], an improved form of the Euler–Knopp transformation has been used. Applied to the series (28) of the scaled velocity $u(y)$, the transformation of Gabutti and Lyness gives

$$u(y) = \sum_{n=0}^{\infty} \frac{n!}{(1-p)^{n+1}} \left(\sum_{j=0}^{n} \frac{(-p)^{n-j}}{(n-j)!j!} A_j y^j \right), \tag{38}$$

Here p is a *tuning parameter* which can be chosen at convenience (for p = –1 one recovers the classical Euler–Knopp type transformation). All the other series equations of Sect. 3 can be transformed similarly. In order to check the convergence of the initial and of the transformed series for specified values of the parameters involved, it is useful to plot their respective terms in the increasing order of the summation indices. This procedure provides at the same time information about the number of terms which has to be considered for a required accuracy of the results.

In addition to "convergence-tuning" with the aid of the transformation (38), the re-formulation of our basic two point boundary value problem (22), (23) into the initial-value problem (22), (35) with the additional condition (34), also offers a powerful tool for a straightforward validation of the results obtained by series summations (since for initial value problems, highly efficient library programs are available). The present paper has made use of all the above numerical procedures in the validation of the results presented.

5 Summary and conclusions

In the present paper buoyant MHD flows with simultaneous Joulean and viscous heating effects were considered in a

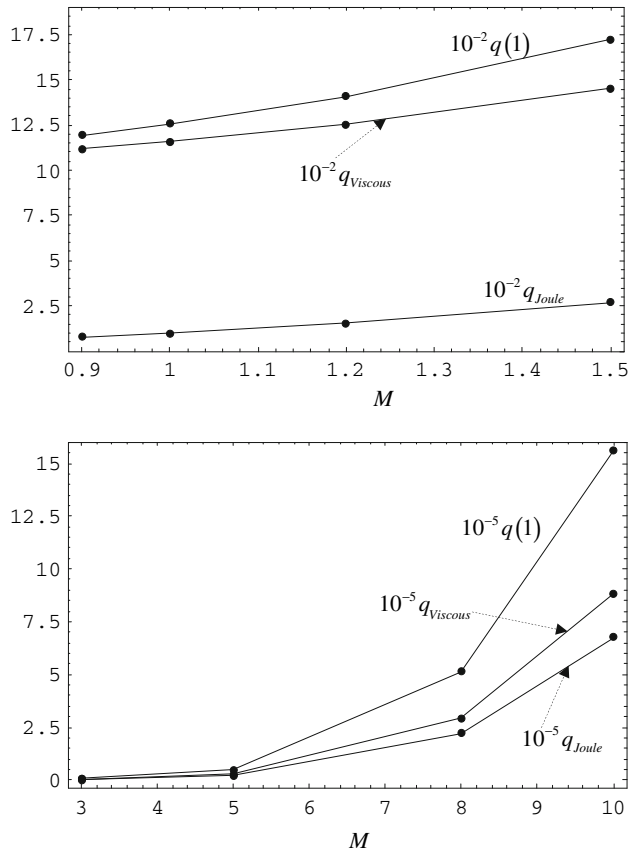

Fig. 6 **a** Shown are the terms of the heat flux balance equation $q(1) = q_{\text{Joule}} + q_{\text{viscous}}$ obtained from (26) and (27) (and multiplied by 10^{-2}) for $M = 0.9,1.0,1.2$ and 1.5. **b** Shown are the terms of the heat flux balance equation $q(1) = q_{\text{Joule}} + q_{\text{viscous}}$ obtained from (26) and (27) (and multiplied by 10^{-5}) for $M = 3$, 5, 8 and 10

vertical parallel plate channel subject to *adiabatic* and *isothermal* boundary conditions, and to a uniform magnetic field applied in a transversal direction. The main concern of the paper was the *levitation regime* of the flow, i.e., the fully developed parallel flow regime for large values of the Hartmann number M with vanishing hydrodynamic pressure gradient. The results can be summarized as follows.

1. The velocity of the flow is directed everywhere downward and for all values of M.
2. In the neighborhood of the left wall, the curvature of the velocity profile is vanishing for all values of M, according to the boundary condition $u''(0) = 0$ (see Fig. 3a, b).
3. For small values of M, the velocity field "fills" the whole channel, nearly symmetrically with respect to the mid-plane (see Fig. 3a). Due to the adiabatic wall condition $(dT/dY|_{Y=0} = 0)$, in an infinitesimal neighborhood of the left wall the fluid temperature is unchanged (horizontal tangent, Fig. 4a) and thus the buoyancy is non-effective here. The buoyancy forces start to act only at finite distances y, driving the fluid in downward direction (negative temperature gradient, Fig. 4a). The magnetic force, as well as the internal heat generation tend to decelerate the downward motion of the fluid.
4. For large values of M, the magnetic force tends to inhibit the downward motion of the fluid. As a consequence, the fluid levitates over a broad transversal range of the channel (Fig. 3b), the motion being constrained into a narrow boundary layer in the neighborhood of the "cold" isothermal wall (Fig. 3b) where the downward pointing buoyancy forces dominate. This confinement of the motion in a thin boundary layer is a manifestation of a general MHD effect with important energy engineering applications.
5. Within the thin boundary layer next to the right wall, the volumetric heat generation both by Joule effect and by viscous friction increases rapidly with increasing values of M, the latter effect being even larger than the former one for all values of M. As a consequence, with increasing M, both the heat transfer rate and the volumetric flow rate increase across the boundary layer steeply.

The extension of the present work for non-vanishing values of the hydrodynamic pressure gradient and non-vanishing incoming heat fluxes $\bar{q}(0)$ is the objective of a current research work.

Acknowledgments One of the authors (E.M.) expresses his gratitude to the *Ministero Italiano dell'Università e della Ricerca* for supporting his collaboration in a *Progetto di Ricerca di Rilevante Interesse Nazionale* concerning the convection heat transfer in internal flows.

6 Appendix A: Case $M = 0$

Using the dimensionless variables $\tilde{y} = Y/L, \tilde{u}(y) = U(Y)/U_0$, the velocity boundary value problem (12), (7), (13), (14) reduces in the case $M \to 0$ to

$$\tilde{u}'''' = \tilde{u}'^2, \tag{39}$$

$$\tilde{u}(0) = 0, \quad \tilde{u}(1) = 0, \quad \tilde{u}''(0) = 0, \quad \tilde{u}'''(0) = 0 \tag{40}$$

Similarly to the case $M \neq 0$, the two-point boundary value problem (39), (40) can be viewed as an initial value problem for (39) with the initial conditions

$$\tilde{u}(0) = 0, \quad \tilde{u}'(0) = \tilde{\alpha}, \quad \tilde{u}''(0) = 0, \quad \tilde{u}'''(0) = 0 \tag{41}$$

whose solution is subject to the additional condition $\tilde{u}(1) = 0$. The Taylor series solution of this problem is given by the following equations

$$\tilde{u}(\tilde{y}) = \sum_{n=0}^{\infty} C_n \tilde{y}^n \tag{42}$$

$$C_{n+4} = \frac{\sum_{j=0}^{n} (j+1)(n-j+1) C_{j+1} C_{n-j+1}}{(n+1)(n+2)(n+3)(n+4)}, \quad n = 0, 1, 2, \ldots \tag{43}$$

where

$$C_0 = 0, \quad C_1 = \tilde{\alpha}, \quad C_2 = 0, \quad C_3 = 0 \tag{44}$$

Equations (45) and (46) imply that all the coefficients of the expansion (42) are vanishing except for C_{3n+1}, n = 0,1,2,.... Thus, the first non-vanishing coefficients are

$$C_1 = \tilde{\alpha}, \quad C_4 = \frac{\tilde{\alpha}^2}{4!}, \quad C_7 = \frac{2\tilde{\alpha}^3}{7!},$$
$$C_{10} = \frac{24\tilde{\alpha}^4}{10!}, \quad C_{13} = \frac{384\tilde{\alpha}^5}{13!}, \ldots \tag{45}$$

The value of the parameter $\tilde{\alpha}$ has to be determined from the second boundary condition (40) which transcribes to

$$\tilde{u}(1) = \sum_{n=0}^{\infty} C_n = \sum_{n=0}^{\infty} C_{3n+1} = 0 \tag{46}$$

With the aid of the Lagrange expansion of implicit functions, (46) can explicitly be solved for the slope parameter $\tilde{\alpha}$. The resulting equation

$$\tilde{\alpha} = -24 \left[1 + \sum_{n=1}^{\infty} \frac{(-24)^{n-1}}{n!} \frac{d^{n-1}}{d\tilde{\alpha}^{n-1}} \left(\sum_{j=7}^{\infty} \frac{A_j}{\tilde{\alpha}} \right)^n \Bigg|_{\tilde{\alpha}=-24} \right], \tag{47}$$

yields the (unique) solution $\tilde{\alpha} = -28.8781$. The corresponding velocity profile (42), is shown in Fig. 3a. We mention that a boundary value problem resembling (39), (40), has been solved by similar methods in [12].

References

1. Poots G (1961) Laminar natural convection flow in magnetohydrodynamics. Int J Heat Mass Transfer 3:1–25
2. Setayesh A, Sahai V (1990) Heat transfer in developing magnetohydrodynamic Poiseuille flow and variable transport properties. Int J Heat Mass Transfer 33:1711–1720
3. Umavathi JC (1996) A note on magnetoconvection in a vertical enclosure. Int J Non-Linear Mech 31:371–376
4. Umavathi JC, Malashetty MS (2005) Magnetohydrodynamic mixed convection in a vertical channel. Int J Non-Linear Mech 40:91–101
5. Bühler L (1998) Laminar buoyant magnetohydrodynamic flow in rectangular ducts. Phys Fluids 10:223–236
6. Burr U, Müller U (2001) Rayleigh–Bénard convection in liquid metal layers under the influence of a vertical magnetic field. Phys Fluids 13:3247–3257
7. Gelfgat A Yu, Bar-Yosef PZ (2001) The effect of an external magnetic field on oscillatory instability of convective flows in a rectangular cavity. Phys Fluids 13:2269–2278
8. Sposito G, Ciofalo M (2006) One-dimensional mixed MHD convection. Int J Heat Mass Transfer 49:2939–2949
9. Knopp K (1990) Theory and application of infinite series. Dover, New York
10. Gabutti B, Lyness JN (1986) Some generalizations of the Euler–Knopp Transformation. Numer Math 48:199–220
11. Morton BR (1960) Laminar convection in uniformly heated vertical pipes. J Fluid Mech 8:227–240
12. Barletta A, Magyari E, Keller B (2005) Dual mixed convection flows in a vertical channel. Int J Heat Mass Transfer 48:4835–4845